A Higher Order Panel Method Applied to Vortex Sheet Roll-Up

H. W. M. Hoeijmakers* and W. Vaatstra†
National Aerospace Laboratory NLR, Amsterdam, The Netherlands

The paper describes a computational method for two-dimensional vortex sheet motion in incompressible flow. The procedure utilizes a second-order panel method, an adaptive panel scheme, and a concept for treating highly rolled-up portions of the vortex sheet. Results are presented for the roll-up of the wake behind an elliptically loaded wing, a ring wing (nacelle), a fuselage/part-span flap/wing combination, and a delta wing with leading-edge vortex sheets. The examples demonstrate that the method is capable of describing complicated vortex sheet motion in a reliable and stable manner.

Nomenclature

C_v^i	= ith segment of vortex sheet
COV	= center of vorticity
E_1, E_2, E_3	= expressions in influence of doublet distribution
e_n	= unit normal vector
e_t	= unit tangential vector
e_x	= unit vector along x axis
i	= vortex sheet segment number
k_n	= curvature
L.E.	= leading edge
N	= number of points on vortex sheet segment
NN	= number of points after rediscretization
NP	= number of panels on vortex sheet segment
T.E.	= trailing edge
t	= arc length along vortex sheet
t_j	= value of t at panel edge
$\hat{t}_j$	= panel midpoint
t_j^*	= panel expansion point
U_d	= velocity induced by doublet distribution
U_∞	= freestream velocity
V_j, W_j	= velocity components in crossflow plane
$X(t)$	= $(0, Y(t), Z(t))$ parametric description of vortex sheet
X_v	= $(0, Y_v, Z_v)$ position vector of vortex
X_0	= position vector of collocation point
x,y,z	= Cartesian coordinates
Y_j, Z_j	= panel-edge point on vortex sheet segment
Γ	= strength of vortex core
θ	= angular extent of vortex sheet
θ_{max}	= maximum angular extent of panel
$\rho(t)$	= doublet distribution
ρ_j	= value of doublet distribution at panel edge
τ	= time-like coordinate x/U_∞
τ_0	= initial time of computation
Δ	= average panel width
Δ_{max}	= maximum panel width
Δt_j	= panel width
$\Delta\tau$	= time step

Introduction

THE evolution of unsteady two-dimensional vortex sheets is of fundamental importance in understanding the large-scale behavior of two-dimensional, quasi-two-dimensional and in many cases of three-dimensional thin shear layers in a variety of fluid mechanical applications. Examples are the flowfield behind the trailing edge of wings, the flow above wings with highly swept leading edges, the flow about slender bodies at high angle of attack, and the flowfield behind propellers and wind turbines. In this paper attention is focussed on the roll-up of the vortex wake behind wings in incompressible flow. Although viscosity is responsible for the formation of the shear layer forming the wake, the behavior of the shear layer can be described in a first approximation by potential flow calculations. In such calculations the shear layer, in the limit of infinite Reynolds number, is shrunk into a doublet (vorticity) distribution on a sheet in an otherwise irrotational flow. The problem of determining the location of the three-dimensional steady vortex sheet is simplified by considering the sheet to be two-dimensional in the crossflow plane and unsteady by replacing the streamwise coordinate x with $U_\infty\tau$, where τ is a time-like coordinate (Fig. 1). The assumptions imply that the trailing vortex sheet is only mildly curved in the streamwise direction and that there is no direct influence from the upstream wing generating the sheet. This seems to be justified sufficiently far downstream of the trailing edge. The problem is then reduced to an initial value problem describing the motion of the vortex sheet as it is convected with the local flow velocity in subsequent crossflow planes. The initial conditions of the problem are the shape of the trailing (shedding) edge of the wing and the distribution of the vorticity shed at this edge.

In the past there have been a large number of attempts to model the vortex sheet motion by replacing the continuous vortex sheet with a finite number of discrete vortices or, alternatively, by replacing the doublet sheet with segments carrying a piecewise constant doublet distribution. Rosenhead[1] was the first to attempt this approach with an analysis of the nonlinear Kelvin-Helmholtz instability in a two-dimensional vortex sheet of constant strength. Westwater[2] first applied the discrete vortex method to the problem of vortex wake roll-up behind an elliptically loaded wing. Attempts to improve upon Westwater's results by increasing the number of vortices representing the vortex sheet have not been successful. It appeared that this approach inevitably led to chaotic motion in the region of the tip vortex, which resulted in loss of the identity of the vortex sheet. Different approaches have been attempted to regularize the solution, such as introducing a finite core for the vortices in which the velocity remains finite,[3,4] using a process of amalgamation in which the vortices are combined if they approach each other too closely or if they have to represent too large a part of a turn in a spiraling sheet,[5] or employing the so-called sub-vortex technique.[6] However, it appears that despite these various attempts the discrete vortex representation results inevitably in numerical instabilities, i.e., chaotic motion, when the number of vortices is increased or the core radius is decreased. For the case of wing tip vortices the so-called method of rediscretization, put forward by Fink and Soh,[7] has been the most successful in obtaining smooth vortex sheet behavior with spiral-type roll-up over longer periods than have been reported previously. However, recent investigations by Baker[8] into the stability of the rediscretization method for the case of double-branched spiraling vortex sheets demonstrate that this method eventually ends in chaos as well.

An alternative approach to the present problem is the so-called cloud-in-cell method as employed by Baker.[9] In this

Presented as Paper 82-0096 at the AIAA 20th Aerospace Sciences Meeting, Orlando, Fla., Jan. 11-14, 1982; submitted Jan. 25, 1982; revision received July 6, 1982.

*Research Engineer, Fluid Dynamics Division. Member AIAA.
†Research Engineer, Informatics Division.

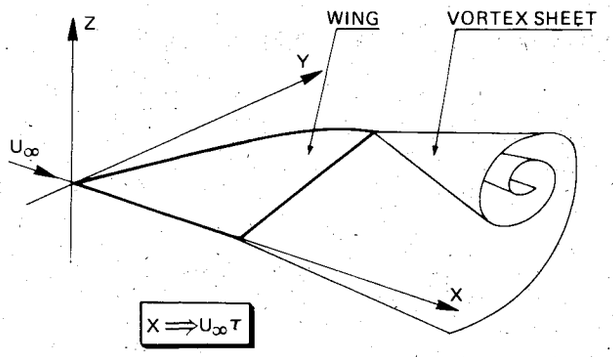

Fig. 1 Rolling-up vortex wake.

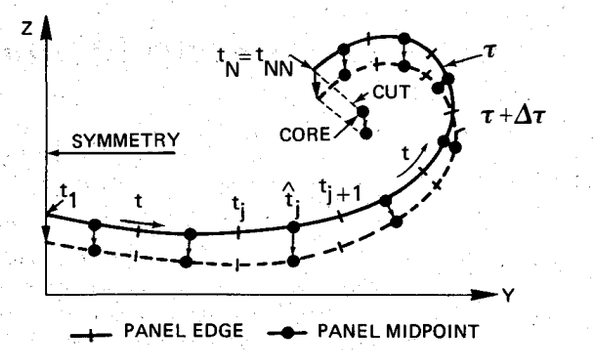

Fig. 2 Vortex sheet arrangement.

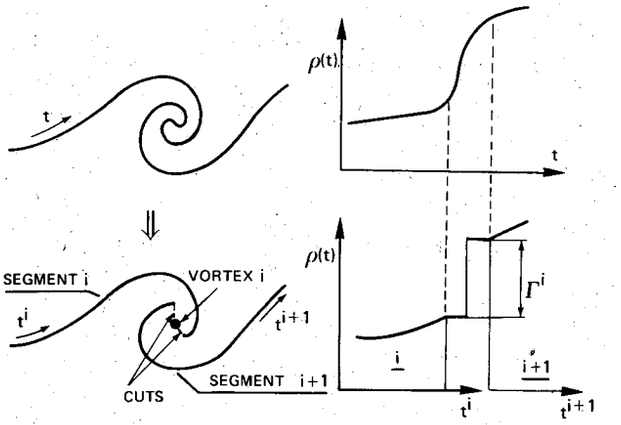

Fig. 3 Concept of double-branched vortex.

method the velocity field due to the discrete vortices is computed by solving Poisson's equation for the stream function due to a grid-dependent region of distributed vorticity in the two-dimensional plane (using a fast Poisson solver). The main disadvantages of this method are that the definition of the sheet is lost and that a large number of grid-dependent small-scale structures appear for which the relevance to the large-scale roll-up process is difficult to assess. For a more comprehensive review, see Ref. 10. However, at present it appears that the discrete-vortex method is not adequate to compute vortex wake roll-up reliably or smoothly. It must be noted here that the question of the existence and uniqueness of the solutions for equations describing vortex sheet motion has not yet been fully resolved. Moore[11] has put forward mathematical arguments demonstrating the possibly ill-posedness of the present initial value problem.

The objective of the present investigation is to demonstrate that a more reliable method for tracking vortex sheet motion is obtained by using a more accurate representation of the deforming vortex sheet, i.e., by replacing the discrete vortex (= vortex lattice) method with a second-order panel method.

Description of the Method

Computing the motion of vortex sheets is complicated by the occurrence of regions where the sheet tends to roll up. In highly rolled-up regions the closely spaced turns of the spiraling sheet represent a region of continuously distributed vorticity, i.e., a vortex core. Although in the present method each of these turns is represented by a sufficient number of elements (panels), it is more appropriate to represent such regions by a simple isolated vortex at the center of vorticity of the spiral (Fig. 2). The vortex is connected to the remainder of the sheet by cuts (feeding sheets). This representation for the inner portion of a spiral vortex sheet has been used by Smith[12] in the case of the leading-edge vortex core above slender delta wings and also by Pullin in his study of similarity solutions for wing tip vortices and double-branched spiral vortices (Refs. 13 and 14, respectively). A more sophisticated method of incorporating the effect of rotational cores into vortex sheets may be that introduced by Huberson,[15] where the inviscid rotational flow inside the core is simulated by a region with a continuous vorticity distribution.

For the method proposed here, the basic computational scheme will be outlined, followed by a more detailed description of the more important parts of the scheme. The basic scheme is:

1) From a given position and strength of the sheet at time τ, defined by the values of Y_j, Z_j, and ρ_j for $j=1(1)N$ at discrete points (Fig. 2), a cubic spline approximation is computed which yields $Y(t)$, $Z(t)$, and $\rho(t)$.

2) The sheet increases in length as it stretches in time. To control the length of the sheet, the sheet is cut to a specified length or, alternatively, it is cut such that its angular extent does not exceed a specified amount. If the sheet is cut, the vorticity contained in the cutoff piece is dumped into the vortex, which is subsequently placed at the center of vorticity of the original vortex and the cutoff piece of the sheet.

3) With the cubic spline representation for $Y(t)$ and $Z(t)$ an adaptive curvature-dependent point distribution t_j, $j=1(1)NN$ is computed such that $\Delta t_j = t_{j+1} - t_j = \Delta_{\max}$ unless Δt_j spans an arc of more than $\theta_{\max}$ degrees of a circle with a radius equal to the average radius of curvature within $[t_j, t_{j+1}]$. In the latter case $t_j = \theta_{\max}/k_n$, where k_n is the average curvature in the interval. The values of Y_j, Z_j, and ρ_j for $j=1(1)NN$ are computed from the spline representation.

4) The discrete values of Y_j, Z_j, and ρ_j for $j=1(1)NN$ are the input for the panel method which computes the velocity components (V_j, W_j) at the panel midpoints $\hat{t}_j = (t_j + t_{j+1})/2$ to second-order accuracy.

5) The panel midpoints are advanced in time by a simple Euler scheme, i.e., by an amount $(V_j \Delta\tau, W_j \Delta\tau)$ where $\Delta\tau$ is chosen such that each midpoint $\hat{t}_j$ is not displaced by more than a specified fraction of Δt_j. The new position of the end points t_1 and t_{NN} are found by quadratic extrapolation from the new values at the three nearest midpoints. Also the position of the isolated vortices is advanced by the local velocity times the time step (Fig. 2).

6) The new values of Y and Z at $\hat{t}_j$ and at t_1 and t_{NN} are the input data for a quadratic spline procedure which computes the new values of Y and Z at the points t_j, $j=1(1)NN$. Subsequently steps 1-6 are repeated with the new Y_j, Z_j, and conserved values ρ_j.

It should be noted here that in step 1, where the data are given at nodal points, interpolatory cubic splines are used primarily for reasons of numerical (spline) stability. Because in step 6 the data are given at midpoints, interpolatory quadratic splines are employed for the same reason. The accuracy of both spline representations is such that the second-order accuracy is maintained.

Treatment of Highly Rolled-Up Regions

In computing the evolution of two-dimensional vortex sheets, two types of rolled-up regions occur. The first appears

at locations where for $\tau=0$ the doublet distribution is singular, such as at a wing tip where $\rho(t)\sim\sqrt{2\epsilon}$, ϵ being the distance from the tip. If a second-order panel method is used to compute the velocity field induced by a doublet distribution with such behavior, large errors appear near the wing tip[16] and no smooth roll-up behavior can be expected. In view of this it seems appropriate to use Pullin's[13] self-similar solution for the rolling up of a semi-infinite vortex sheet to construct a suitable initial solution for $\tau=\tau_0$. Here τ_0 is small compared to the time scale for which the development of the vortex sheet at the tip is strongly influenced by other parts of the sheet.

A second type of highly rolled-up region may appear at locations where the vortex sheet is initially smooth and the doublet distribution nonsingular. Examples of this occur in the wake of delta and ring wings and in the wake behind wings with deployed part-span flaps. Using the adaptive panel scheme, the number of panels increases rapidly in such a sheet region because of stretching and increasing curvatures. While more and more detail of the double-branched spiral develops, the time step $\Delta\tau$ allowed decreases as a result of the decreasing panel sizes in the affected region. Thus, the computation ceases to progress significantly in τ. As with the wing tip vortex, it is argued here that (for the outer flow) the highly rolled-up region may be represented by an isolated vortex placed at the center of vorticity and connected by cuts to the remainder of the sheet (Fig. 3). In this way a vortex sheet is split into two segments and eventually a vortex sheet with multiple segments and multiple isolated vortices evolves quite naturally. Since the region of highest curvature has now been eliminated, the time step allowed is increased and the computation proceeds more rapidly in τ.

Panel Method

In the present investigation a second-order panel method is used to compute the velocity field induced by the multiple-segmented vortex sheet. It is suggested that the use of a method more accurate than the discrete-vortex method to compute the velocity field precludes the appearance of instabilities in the vortex sheet due to the spurious numerical effects introduced by a too crude representation. Results of an earlier attempt in this direction by Mokry[17] using a first-order panel method seemed promising, but numerical instabilities still appeared, especially in the case of a wing with a part-span flap. The vortex sheet is represented by a doublet distribution. The velocity induced by a doublet distribution $\rho(t)$ on a sheet with segments C_v^i in incompressible flow is written as

$$U_d(X_0)=-\frac{1}{2\pi}\boldsymbol{e}_x\times\sum_i\left(\int_{C_v^i}\frac{\mathrm{d}\rho^i}{\mathrm{d}t}\frac{\boldsymbol{R}}{|\boldsymbol{R}|^2}\,\mathrm{d}t - [\rho^i(t_{NN})-\rho^{i+1}(t_1)]\frac{\boldsymbol{R}_v}{|\boldsymbol{R}_v|^2}\right) \tag{1}$$

where superscript i denotes the functions on the ith segment, $\boldsymbol{R}=X_0-X^i(t)$, and $\boldsymbol{R}_v=X_0-X_v^i$. The second term in Eq. (1) results because the doublet distribution is continued as a constant on the cuts and has a jump (equal to the strength of the vortex) across the vortex position (Fig. 3). The curve C_v^i is divided into NP panels. On each panel the functions $\rho^i(t)$, $Y^i(t)$, and $Z^i(t)$ are approximated by piecewise quadratic representations. To evaluate the integral in Eq. (1) to second-order accuracy a similar approach is followed by Hess,[18] i.e., a small-curvature expansion about an expansion point (the point $\hat{t}_j$ in Ref. 18) $t_j^*\in[t_j,t_{j+1}]$. Writing on each panel and dropping the superscript (Fig. 4),

$$\rho'(t)=\rho'(t_j^*)+(t-t_j^*)\rho''(t_j^*)+0(\Delta t_j^2) \tag{2a}$$

$$X(t)=X(t_j^*)+(t-t_j^*)X'(t_j^*)+\tfrac{1}{2}(t-t_j^*)^2X''(t_j^*)+0(\Delta t_j^3) \tag{2b}$$

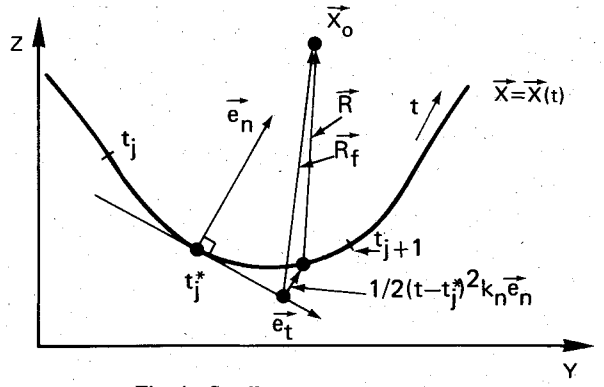

Fig. 4 Small-curvature expansion.

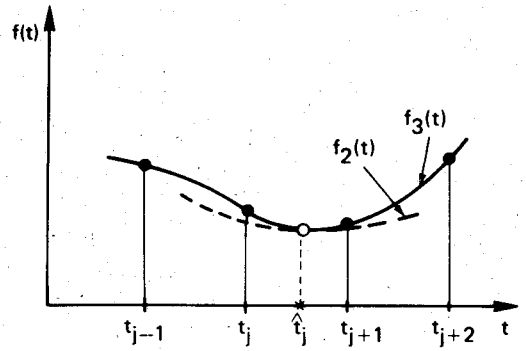

Fig. 5 Quadratic representation $f_2(t)$.

one obtains

$$\boldsymbol{R}=\boldsymbol{R}_f-\tfrac{1}{2}(t-t_j^*)^2k_n\boldsymbol{e}_n+0(\Delta t_j^3) \tag{2c}$$

where $\boldsymbol{R}_f$ is the distance from X_0 to the point t on the flat-panel approximation of the panel and k_n is the curvature, i.e., $k_n=X'(t_j^*)\times X''(t_j^*)\cdot\boldsymbol{e}_x$ at the expansion point. In Eq. (2c) the unit normal which is given by $\boldsymbol{e}_n=\boldsymbol{e}_x\times X'(t_j^*)$ and $\boldsymbol{e}_t$, the unit vector tangential to C_v at t_j^*, is given by $\boldsymbol{e}_t=X'(t_j^*)$. Assuming that k_n is not too large, the integral in Eq. (1) can be expressed as

$$\sum_{j=1}^{NP}\{\rho'(t_j^*)(E_1+k_nE_2)+\rho''(t_j^*)E_3\}+0(\Delta^2) \tag{3}$$

where E_1, E_2, and E_3 are expressions involving integrals that can be evaluated in closed form. The expansion point t_j^* is chosen either as the panel midpoint $\hat{t}_j$ for points X_0 not too close to the panel or as the point on the panel nearest to X_0. For points X_0 in the far field of the panel computing time is saved by using a single-pole expansion[18] rather than the small-curvature expansion. It can be shown that with this approach second-order accuracy is maintained.

To avoid spurious effects from the panel edges where the panelwise representations for the geometry and doublet distribution may be discontinuous, the panel midpoints are chosen as those points where the velocity is computed. In examining the expressions for the normal and tangential velocity components induced at $\hat{t}_i$, it is found that these are dominated by a term proportional to $\rho''(\hat{t}_i)$ and $\rho'(\hat{t}_i)$, respectively. This circumstance, typical for the mixed design/analysis character of the boundary conditions in flows with vortex sheets, makes it impossible to use quadratic spline-type representations for $\rho(t)$, $Y(t)$, and $Z(t)$ based on function values at the midpoints. This is because these representations are unstable for prescribing the first derivative at the midpoints. The quadratic representation $f_2(t)$

used in the present method is based on finite difference considerations, is discontinuous in function value as well as first and second derivatives across the panel edges, and has the function values at panel edges as parameters. It is obtained by writing for $t\in[t_j,t_{j+1}]$ (Fig. 5)

$$f_2(t)=f_3(\hat{t}_j)+(t-\hat{t}_j)f_3'(\hat{t}_j)+\tfrac{1}{2}(t-t_j)^2 f_3''(\hat{t}_j) \qquad (4)$$

where $f_3(t)$ is the cubic fitted through the function values at t_{j-1}, t_j, t_{j+1}, and t_{j+2} so that $f_3(\hat{t}_j)$, $f_3'(\hat{t}_j)$, and $f_3''(\hat{t}_j)$ can be written as a linear (finite difference) expression of $f(t)$ at t_{j-1}, t_j, t_{j+1}, and t_{j+2}. The discontinuities in function value, the first and second derivatives of $f_2(t)$ across the panel edges are small (of higher order) and may be neglected. It has been verified that the f_2 representation is stable for prescribing the first and second derivatives at the panel midpoints and the appropriate conditions at t_1 and t_{NN}. It has been used with success for the problem of conical flow about delta wings with leading-edge vortex sheets.[19]

Rediscretization

To maintain the accuracy of the spatial discretization for a stretching vortex sheet, periodic rediscretization[7] is necessary. For the same reason the discretization scheme has to be refined in regions where large variations in the geometry or doublet distribution appear during the computation. To accommodate these requirements, the adaptive curvature-dependent panel scheme described above is used at each time step. The basic panel size Δ_{max} is chosen such that the desired degree of accuracy in regions where no large variations occur is ensured. The second parameter θ_{max} then ensures that at highly curved parts of the sheet the panel size is reduced so that in each region accuracy is maintained. Usually θ_{max} is chosen such that a circle having a radius equal to the radius of curvature is represented by 12-18 panels.

By monitoring such invariants of the evolution process as the total amount of vorticity and the lateral position of the center of vorticity (COV), it has been verified that the present procedure does not significantly accumulate errors.

Applications

In this section four applications, also treated in the literature, are described. For all cases it is assumed that the vortex sheet is symmetric with respect to the $Y=0$ plane so that only the starboard side of the configuration need be considered.

The computing time requirements for the method on the NLR Cyber 73-28 are approximately $6.2\times10^{-4}\ NP^2+1.6\times10^{-2}\ NP$ CPU seconds per time step. The NP^2 term, which for the cases treated here accounts for up to 90% of the computing time, is solely due to the panel method. It is noted in passing that techniques are being developed for reducing the operational count to order NP (e.g., see Ref. 20) which hold the promise of considerably reducing the computational effort required.

Elliptically Loaded Wing

The case of the elliptically loaded wing, for which initially

$$\rho(t)=(1-t^2)^{1/2},\quad Y(t)=t,\quad Z(t)=0 \qquad (5)$$

for $t\in[0,1]$, is classically used for testing vortex sheet roll-up procedures. The present second-order method cannot handle the singular behavior near the tip $t=1$; thus a regular starting solution is required. For this purpose Pullin's[13] self-similar solution for the semi-infinite vortex sheet problem (Kaden's problem), defined as $\rho(t)=2(1-t)^{1/2}$, $Y(t)=1-t$, and $Z(t)=0$ for $t\in[-\infty,1]$ at $\tau=0$, is used. In the numerical results presented here, it is assumed that the roll-up has proceeded to a time τ_0 at which point the sheet is undistorted for $t\in[0,0.95]$ and has the self-similar shape for $t>0.95$. Application of the matching conditions at $t=0.95$ determines τ_0 at the value

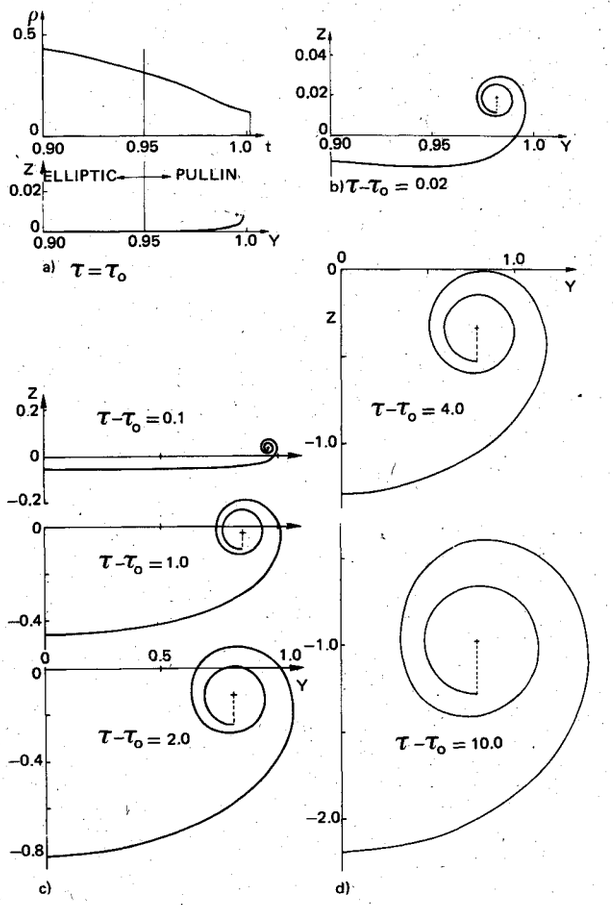

Fig. 6a-d) Elliptically loaded wing: a) $\tau=\tau_0$, b) $\tau-\tau_0=0.02$, c) $\tau-\tau_0=0.1$, 1.0, and 2.0, d) $\tau-\tau_0=4.0$ and 10.0.

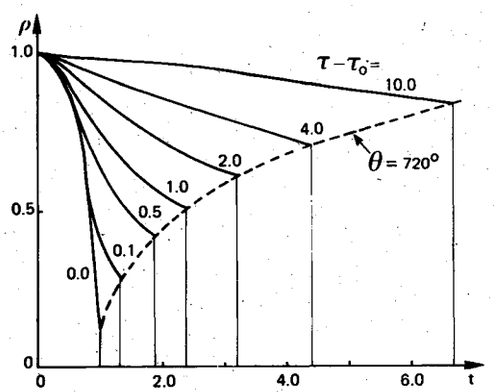

Fig. 6e Doublet distribution for different $\tau-\tau_0$.

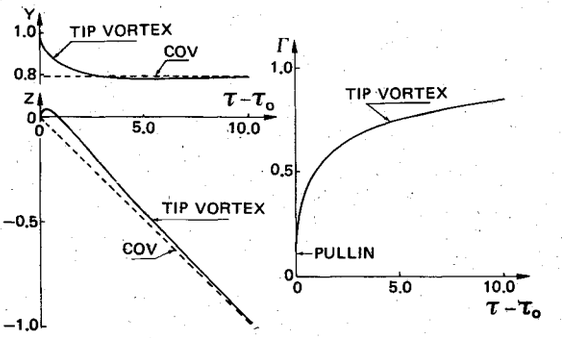

Fig. 6f Position and strength of tip vortex.

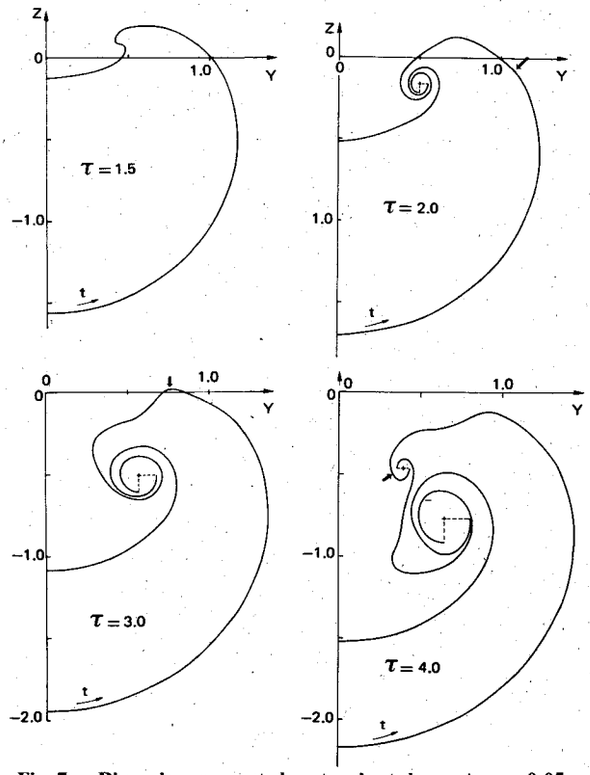

Fig. 7a Ring wing, computed vortex sheet shapes $\Delta_{max} = 0.05$.

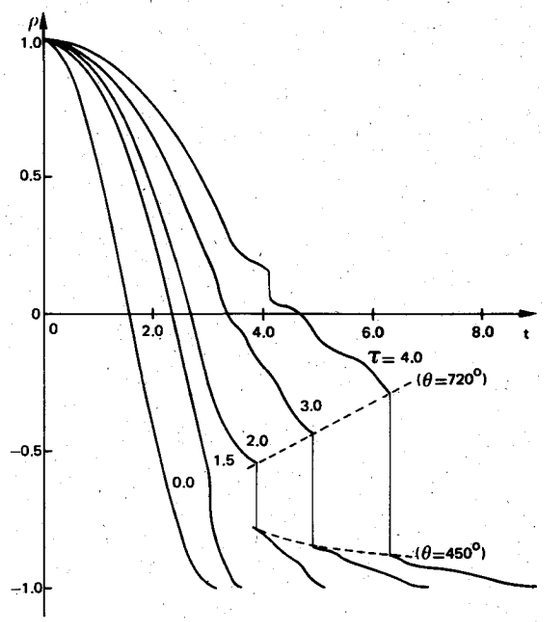

Fig. 7b Doublet distribution for various τ.

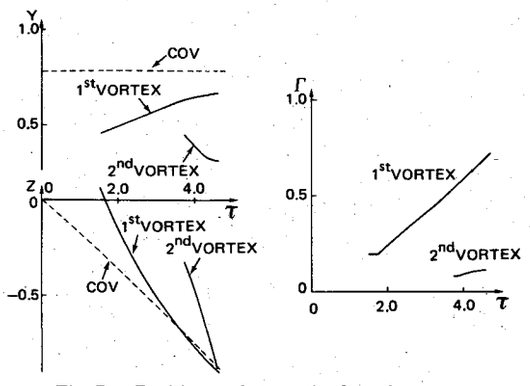

Fig. 7c Position and strength of vortices vs τ.

0.00271. It also determines both the geometry and the doublet distribution of the initial solution. The initial solution for $t > 0.90$ is shown in Fig. 6a. Although Pullin's solution involves more than four complete turns of the sheet, only one-quarter turn is used here. Subsequently the solution of the sheet is computed by letting the sheet roll up from the position of the cut shown at $\theta = 90$ deg for $\tau = \tau_0$ to $\theta = 720$ deg which is reached at $\tau - \tau_0 = 0.00618$. Afterwards the cut is held at this position, each time step cutting off the sheet in excess of $\theta = 720$ deg as described before. In the computation $\theta_{max} = 20$ deg and $\Delta_{max} = 0.01$, 0.02, 0.03, 0.04, 0.05, and 0.1 for $\tau - \tau_0 \in [0,0.0072)$, $[0.0072,0.063)$, $[0.063,0.094)$, $[0.094,0.148)$, $[0.148,5.05)$, and $[5.05,10.0]$, using 238, 200, 300, 100, 1400, and 500 time steps, respectively. The number of panels used varied between 55 and 136. The shape of the outer part of the sheet at $\tau - \tau_0 = 0.02$ is shown in Fig. 6b, which is similar to Pullin's[13] solution. Figure 6c shows the computed shapes for $\tau - \tau_0 = 0.1$, 1.0, and 2.0, demonstrating that smooth solutions are obtained. These solutions are nearly identical to those obtained by Moore[5] and Fink and Soh.[7] The computed shapes for longer times, namely $\tau - \tau_0 = 4.0$ and 10.0, are presented in Fig. 6d. At $\tau - \tau_0 = 10.0$ the turns around the vortex clearly become more elliptic in shape due to the mutual influence of the starboard and port vortices. Note that there is no sign of developing instabilities, which, presumably, is related to the fact that in this case the sheet is stretching everywhere during the computation. In Fig. 6e the doublet distribution is plotted vs the arc length t for different $\tau - \tau_0$. It shows that the strength $\Gamma = \rho(t_N)$ of the tip vortex increases rapidly, so that at $\tau - \tau_0 = 1.0$ the vortex contains 50% of the vorticity. Finally in Fig. 6f the positions of the core, COV, and the vortex strength are plotted as functions of $\tau - \tau_0$. It indicates that initially the vortex moves rapidly upward and inboard and that for longer times the vortex and COV position tend to coincide, as should be expected.

The theoretical COV lateral position $\pi/4$ quite accurately predicted an error of less than 1% at $\tau - \tau_0 = 10$. The slope of the vertical position, which theoretically tends to $1/\pi^2$ for large τ, is also quite accurately predicted.

Ring Wing or Nacelle

The case of the vortex wake of a ring wing or nacelle is of interest because initially both the doublet distribution and the geometry are regular. At $\tau = 0$ one has

$$\rho(t) = \cos(t), \quad Y(t) = \sin(t), \quad Z(t) = -\cos(t) \qquad (6)$$

for $t \in [0,\pi]$. This case has been treated by Baker[8] with the method of Fink and Soh[7] and by Baker[21] with the "cloud-in-cell" method. Results of the present investigation, with $\Delta_{max} = 0.05$, $\theta_{max} = 20$ deg using 1170 time steps and between 63 and 227 panels are shown in Fig. 7. From Fig. 7a it is clear that after some time (here at $\tau = 1.52$) a vortex structure

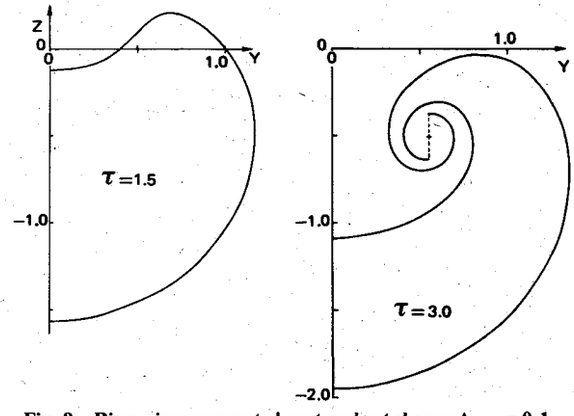

Fig. 8 Ring wing, computed vortex sheet shapes $\Delta_{max} = 0.1$.

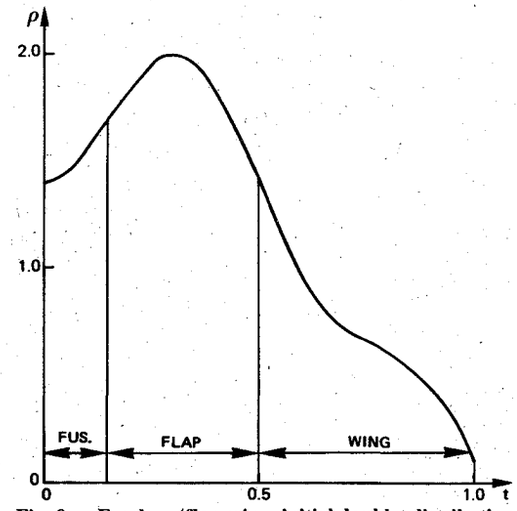

Fig. 9a Fuselage/flap-wing, initial doublet distribution.

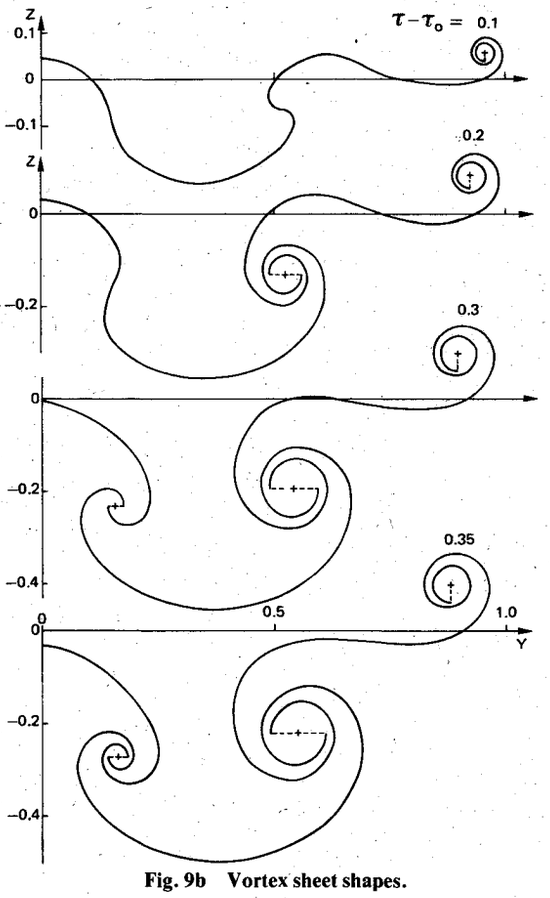

Fig. 9b Vortex sheet shapes.

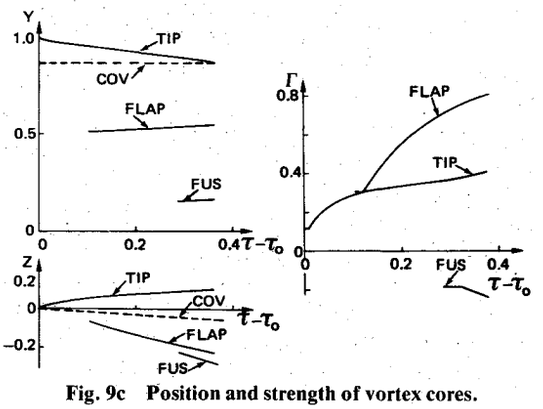

Fig. 9c Position and strength of vortex cores.

evolves which resembles the tip vortex of the preceding case. The appearance of this (double-branched) vortex is the result of the steepening of the doublet distribution as time proceeds. This is clarified in Fig. 7b, which shows that at a point, originally at $(t/\pi)\times 180 = 130$ deg, the doublet distribution becomes quite steep. In a similar fashion a second (weaker) vortex appears at $\tau = 3.755$, at a point originally at $(t/\pi)\times 180 = 83$ deg. The magnitude of the jump in the distribution corresponds to the strength of the vortex, while the dashed line indicates a fixed position of the cuts as shown in Fig. 7a. The formation of vortices as the result of the steepening of the doublet distribution has some analogy in unsteady transonic flow where shock waves are formed as a result of the steepening of the pressure distribution. The position of the vortices and their strengths as a function of time are shown in Fig. 7c. From this it can be seen that after its appearance the first vortex moves down at a faster rate than the COV, but gradually slows to move at the same downward speed as the COV. The lateral position of the COV is theoretically $\pi/4$, which is predicted with an error of less than 0.5%. It is also seen that for large τ the slope of the vertical position tends to $2/\pi^2$ which would be the sinkage rate for the sheet rolled up into one vortex.

In examining the results of the computation it became clear that vortices do develop in regions where the sheet stretches the least or does not stretch at all. Furthermore, because of the implied smoothing of the computational scheme, a vortex structure can develop only if its length scale is larger than a few times Δ_{max}. This is also demonstrated in Fig. 7a, where the first bump in the shape of the sheet does not develop into a vortex, while the second one, indicated by the arrow, does.

The consequence of this effect is best checked by repeating the computations for different Δ_{max}. The vortex sheet shapes shown in Fig. 8 are computed with $\Delta_{max} = 0.1$. It can be seen that the global picture obtained is the same, but that the bulges apparent in Fig. 7a have been eliminated and a smoother shape evolves. The first vortex appears later, namely at $\tau = 1.88$. Repeating the calculation with $\Delta_{max} = 0.025$ showed that more small-scale details appear but in a much more regular manner than in Ref. 21. The first vortex appears earlier than in the case of Fig. 7, namely at $\tau = 1.32$. These results indicate that aside from the global structure, the details of the computed shapes depend on the amount of smoothing applied. In the present method the smoothing is apparently controlled by the parameter Δ_{max}. Regular small-scale flow structures similar to the present ones have been observed in experiments involving rolling-up shear layers as well. There it appears that structures with a length scale less than a few times the shear-layer thickness are smoothed out and thus not amplified into well-defined rotational cores. Since the shear-layer thickness is related to the Reynolds number, it would be of great interest to attempt to correlate Δ_{max} with the Reynolds number.

The present results also suggest that the initial value problem for the ring wing vortex sheet is ill-posed, i.e., that this vortex sheet (the shear layer for infinite Reynolds number) is inherently unstable. The results of the present method may be viewed as results for a finite Reynolds number, the value of which is related to Δ_{max} in an as yet unknown manner.

Fuselage/Flap-Wing

In the two applications discussed above the vorticity $-\rho'(t)$ was positive everywhere. The next two applications are of interest because the sheet contains vorticity with both positive and negative signs, resulting in counter-rotating vortex cores. First consider the load distribution which schematically represents the case of a wing/fuselage combination with a deployed part-span flap. The doublet distribution is the same as that used by Baker[9] for a similar calculation using the "cloud-in-cell" method (Fig. 9a). It is given in three parts: for

$t \in [0,0.3]$ it is the cubic defined by $\rho(0)=1.4$, $\rho'(0)=0$, $\rho(0.3)=2.0$, and $\rho'(0.3)=0$; for $t \in [0.3,0.7]$ by the cubic with the same data at $t=0.3$ and with $\rho(0.7)=(1-0.7^2)^{1/2}$, $\rho'(0.7)=-0.7/(1-0.7^2)^{1/2}$; for $t \in [0.7,1]$ ρ is elliptic, i.e., $\rho(t)=(1-t^2)^{1/2}$. As for the case of the elliptically loaded wing, Pullin's[13] solution with $\tau_0=0.00271$ is used for the tip region. It is known that a load distribution like the one of Fig. 9a will produce three vortices.[22] The many small-scale structures in the results of Baker[9] make it difficult to identify the sheet and the structure of the rolled-up parts of the sheet. The present results are more definite in this respect and are obtained with $\theta_{max}=20$ deg and $\Delta_{max}=0.01$ for $\tau-\tau_0 \in [0,0.0073)$, $\Delta_{max}=0.02$ for $\tau-\tau_0 \in [0.0073,0.089)$, and $\Delta_{max}=0.03$ for $\tau-\tau_0>0.089$ using between 83 and 183 panels in 1575 time steps. The computed vortex sheet shapes are shown in Fig. 9b. Three vortices evolve: the first is the tip vortex; the second the double-branched "flap" vortex which appears at $\tau-\tau_0=1.056$ and originates near the outboard edge of the flap; and the third is the vortex originating at the inboard edge of the flap, denoted here as the fuselage vortex which is weaker and appears at $\tau-\tau_0=2.895$. Figure 9c shows the positions of the vortices and the COV, as well as the strength of vortices vs $\tau-\tau_0$. The lateral position of the COV is theoretically at 0.8669; the numerically found position is less than 0.5% removed from this value.

In Fig. 9c the short times over which Γ is constant are the periods in which the cuts are allowed to move. If Γ increases in magnitude the cuts are at a fixed attitude and vorticity is fed into the core(s). Note that at $\tau-\tau_0=0.4$ about 60% of the vorticity with a positive sign is contained within the tip and flap vortex and about 30% of the vorticity with a negative sign is contained in the fuselage vortex.

Delta Wing

The final application concerns the wake behind a slender delta wing with a unit aspect ratio (76 deg sweep) at 20.5 deg angle of attack. At this high angle of attack a leading-edge vortex flow develops above the wing. There has been an earlier attempt to compute the shape of the wake for this case[23] using the discrete-vortex method and starting from a guess for the shape of the leading-edge vortex sheet. The vortex sheet method developed by Johnson[24] for the full three-dimensional flow over wings with leading-edge vortex sheets assumes a fixed wake of assumed (unrolled) shape. The effect of this assumption remains to be investigated. Kandil[25] employs a three-dimensional discrete-vortex method to compute the flow and a pattern like that observed by Hummel[26] evolves, but the method experiences problems similar to its two-dimensional counterpart described in the Introduction.

The typical doublet distribution on the wing and vortex sheet for the present case is shown in Fig. 10a. Together with the shape of the leading-edge vortex sheet and the position of the leading-edge vortex core, it is obtained from the conical flow solution.[19] The computation was carried out with $\Delta_{max}=0.05$ and $\theta_{max}=20$ deg using between 64 and 188 panels in 683 time steps. In Fig. 10b the computed shapes at the trailing edge and at 12.5 and 25% root chord behind the trailing edge ($\tau=0$, 0.1875, and 0.375, respectively) are compared with the shapes observed in the wind tunnel of the Delft University of Technology with the laser/light-screen technique. Both results show clearly the development of the so-called trailing-edge vortex[26] which originates at about the 70% semispan location on the trailing edge. The agreement between the two results is quite good.

Note that in the photographs small-scale structures are clearly recognizable in the shear layer, especially at $\tau=0$. In Fig. 10c the position of the vortex cores and the COV and strength of the cores are given as a function of time.

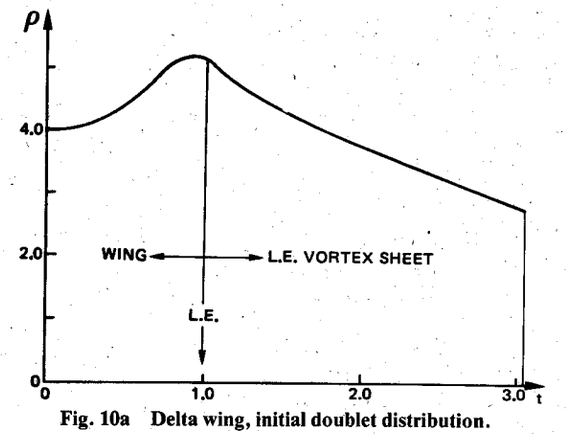

Fig. 10a Delta wing, initial doublet distribution.

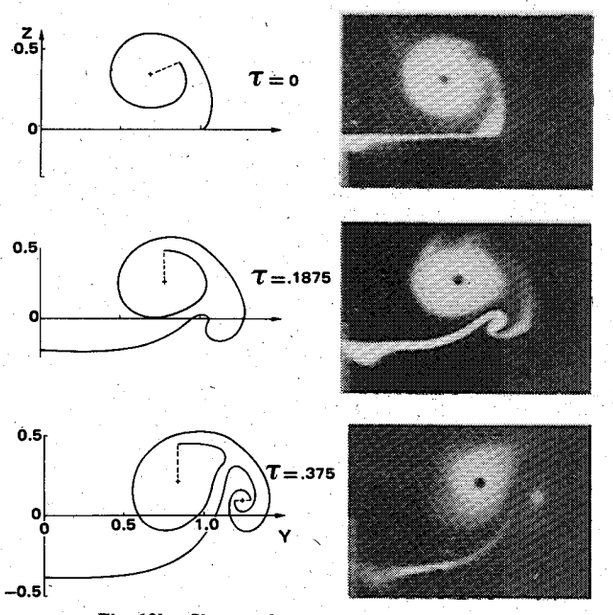

Fig. 10b Shapes of vortex sheet at different τ.

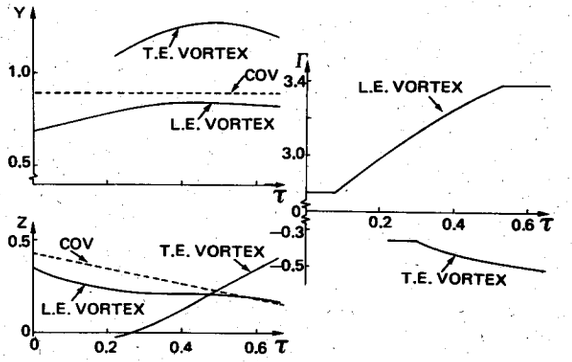

Fig. 10c Position and strength of vortices.

Conclusions

For the problem of two-dimensional vortex sheet motion a computational procedure has been developed which enables vortex sheet motion to be followed in a reliable, stable, and smooth manner for long periods of time (or large distances downstream). The basic elements of the procedure are a second-order panel method for the accurate computation of the velocity field, an adaptive curvature-dependent panel scheme, and the concept for treating highly rolled-up portions

of vortex sheets. In view of the interest in aerodynamics for the evolution of thin shear layers with features much larger than the shear-layer thickness, the significance of the results computed with the present method lies in the fact that the numerical smoothing implied in the method effectively turns the vortex sheet into a thin shear layer. However, the correlation of the smoothing parameter with the effective thickness remains to be investigated.

Acknowledgments

The authors are indebted to Dr. D. I. Pullin of the University of Melbourne, Australia, for providing the self-similar solution to Kaden's problem in tabulated form. We gratefully acknowledge N. G. Verhaagen of the Delft University of Technology, the Netherlands, for providing the laser/light-screen photographs of Fig. 10 and also for his cooperation in filming the results of experiment and computation.

References

[1] Rosenhead, L., "The Formation of Vortices from a Surface of Discontinuity," *Proceedings of the Royal Society of London,* Series A, Vol. 134, 1931, pp. 170-192.

[2] Westwater, F. L., "Rolling Up of the Surface of Discontinuity Behind an Aerofoil of Finite Span," Aeronautical Research Council, R&M No. 1962, 1935.

[3] Chorin, A. J. and Bernard, P. S., "Discretization of a Vortex Sheet, with an Example of Roll-Up," *Journal of Computational Physics,* Vol. 13, 1973, pp. 423-429.

[4] Kuwahara, K. and Takami, H., "Numerical Studies of Two-Dimensional Vortex Motion by a System of Point Vortices," *Journal of Physical Society of Japan,* Vol. 34, Jan. 1973, pp. 247-253.

[5] Moore, D. W., "A Numerical Study of the Roll-Up of a Finite Vortex Sheet," *Journal of Fluid Mechanics,* Vol. 63, Pt. 2, 1974, pp. 225-235.

[6] Maskew, B., "Subvortex Technique for the Close Approach to a Discretized Vortex Sheet," *Journal of Aircraft,* Vol. 14, Feb. 1977, pp. 188-193.

[7] Fink, P. T. and Soh, W. K., "A New Approach to Roll-Up Calculations of Vortex Sheets," *Proceedings of the Royal Society of London,* Series A, Vol. 362, 1978, pp. 195-209.

[8] Baker, G. R., "A Test of the Method of Fink and Soh for Following Vortex Sheet Motion," *Journal of Fluid Mechanics,* Vol. 100, Pt. 1, 1980, pp. 209-220.

[9] Baker, G. R., "The 'Cloud in Cell' Technique Applied to the Roll Up of Vortex Sheets," *Journal of Computational Physics,* Vol. 31, 1979, pp. 76-95.

[10] Saffman, P. G. and Baker, G. R., "Vortex Interactions," *Annual Review of Fluid Mechanics,* Vol. 11, 1979, pp. 95-122.

[11] Moore, D. W., "The Spontaneous Appearance of a Singularity in the Shape of an Evolving Vortex Sheet," *Proceedings of the Royal Society of London,* Series A, Vol. 365, 1979, pp. 105-119.

[12] Smith, J. H. B., "Improved Calculations of Leading-Edge Separation from Slender, Thin, Delta Wings," *Proceedings of the Royal Society of London,* Series A, Vol. 306, 1968, pp. 67-90.

[13] Pullin, D. I., "The Large-Scale Structure of Unsteady Self-Similar Rolled-Up Vortex Sheets," *Journal of Fluid Mechanics,* Vol. 88, Pt. 3, 1978, pp. 401-430.

[14] Pullin, D. I. and Phillips, W. R. C., "On a Generalization of Kaden's Problem," *Journal of Fluid Mechanics,* Vol. 104, 1981, pp. 45-53.

[15] Huberson, S., "Numerical Computation of Flows with Rolled-Up Vortex Sheets," *La Recherche Aérospatiale,* Vol. 3, May 1980, pp. 57-63, (English ed.).

[16] Hoeijmakers, H. W. M., "Aspects of Second- and Third-Order Panel Methods Demonstrated for the Two-Dimensional Flat Plate Problem," National Aerospace Laboratory NLR, Rept. NLR TR 81074 U, 1981.

[17] Mokry, M. and Rainbird, W. J., "Calculation of Vortex Sheet Roll-Up in a Rectangular Wind Tunnel," *Journal of Aircraft,* Vol. 12, Sept. 1975, pp. 750-752.

[18] Hess, J. L., "Consistent Velocity and Potential Expansions for Higher-Order Surface Singularity Methods," McDonnell Douglas Corp., Rept. MDC J691L, 1975.

[19] Hoeijmakers, H. W. M. and Vaatstra, W., "A Higher-Order Panel Method for the Computation of the Flow about Slender Delta Wings with Leading-Edge Vortex Separation," *Proceedings of the Fourth GAMM—Conference on Numerical Methods in Fluid Mechanics,* edited by H. Viviand, Vieweg Verlag, Paris, Oct. 1981, pp. 137-149 (also NLR MP 81053 U, 1981).

[20] Slooff, J. W., "Requirements and Developments Shaping a Next Generation of Integral Methods," Paper presented at IMA Conference on Numerical Methods in Aeronautical Fluid Dynamics, Reading, England, 1981 (also NLR MP 81007 U, 1981).

[21] Baker, G. R., "Studies in Vortex Motion," Ph.D. Thesis, California Institute of Technology, Pasadena, 1977.

[22] Donaldson, C. duP., Snedeker, R. S., and Sullivan, R. D., "Calculation of Aircraft Wake Velocity Profiles and Comparison with Experimental Measurements," *Journal of Aircraft,* Vol. 11, Sept. 1974, pp. 547-555.

[23] Jepps, S. A., "Theoretical Calculations of the Wake Behind a Delta Wing with Leading Edge Separation," British Aerospace, Warton, England, Rept. Ae/A/583, 1978.

[24] Johnson, F. T., Tinoco, E. N., Lu, P., and Epton, M. A., "Three-Dimensional Flow over Wings with Leading-Edge Vortex Separation," *AIAA Journal,* Vol. 15, April 1980, pp. 367-380.

[25] Kandil, O. A. and Balakrishnan, L., "Recent Improvements in the Prediction of the Leading and Trailing Edge Vortex Cores of Delta Wings," AIAA Paper 81-1263, June 1981.

[26] Hummel, D., "On the Vortex Formation over a Slender Delta Wing at Large Incidence," AGARD CP-247, 1979, pp. 15.1-15.17.